Catal Lett (2008) 125:289–295
DOI 10.1007/s10562-008-9543-0

Synthesis and Catalytic Performance of Highly Ordered Ru-Containing Mesoporous Carbons for Hydrogenation of Cinnamaldehyde

Peng Gao · Aiqin Wang · Xiaodong Wang · Tao Zhang

Received: 26 May 2008 / Accepted: 6 June 2008 / Published online: 23 July 2008

Abstract Highly ordered Ru-containing mesoporous carbons (Ru-OMC) were for the first time synthesized by a one-pot method. Comparing with our previously reported Ir-OMC, the Ru precursor must be added after the formaldehyde was consumed by polycondensation with resorcinol to obtain a small particle size. The resultant Ru-OMC samples with different Ru contents were characterized with X-ray diffraction (XRD), N_2 adsorption-desorption, and Transmission electron microscopy (TEM). The results evidenced the formation of highly ordered mesostructure, in which Ru particles were imbedded. The new carbon materials were further evaluated in the selective hydrogenation of cinnamaldehyde (CMA). By comparison with the traditional Ru/AC catalyst, our Ru-OMC samples exhibited much higher activity (2–14-fold) and up to 60% of selectivity to cinnamyl alcohol (CMO).

Keywords Mesoporous carbon · Self-assembly · Ruthenium · Cinnamaldehyde · Cinnamyl alcohol · Hydrogenation

1 Introduction

Carbon materials have been widely used as catalyst supports owing to their large surface areas and rich porosities [1–3]. Compared with commercial carbon materials with microporous structure (e.g., activated carbon), the recently developed mesoporous carbons may present additional advantages in terms of mass transfer and utility of internal surfaces, and therefore attracted intensive research attention [4–6]. Two major synthetic pathways have been developed for mesoporous carbons. One is the hard template strategy [7, 8] which involves synthesis of hard template (such as SBA-15), repetitive filling of the pores with carbon precursor, pyrolysis at a high temperature, and removal of the hard template. Due to the multi steps involved and low yield of the carbon, this method is lack of commercial interest. The other attracting strategy is the soft template approach [9–14], which involves polycondensation of resorcinol and formaldehyde under the presence of a surfactant template. This method not only allows for large-scale production, but also yields ordered mesoporous carbons with various macroscopic forms like films, powders, monoliths, etc. More importantly, catalytically active species could be introduced into the above reaction mixture, which facilitates one-pot synthesis of mesoporous carbon-supported catalysts. In our previous work [15, 16], iridium as well as molybdenum carbide was imbedded in the mesoporous carbons by this one-pot procedure, and the resultant composite exhibited high catalytic activities for hydrazine decomposition. Different from the traditional impregnation, the one-pot method yields intimate contact and strong interaction between the active species and the carbon support, which may give rise to a superior catalytic performance.

In this work, in order to explore further the versatility of this one-pot synthesis method, we made an attempt to synthesize Ru-containing mesoporous carbons (Ru-OMC) since carbon-supported Ru is known as one of the most important catalysts in hydrogenation reactions [17–20].

P. Gao · A. Wang · X. Wang · T. Zhang (✉)
State Key Laboratory of Catalysis, Dalian Institute of Chemical Physics, Chinese Academy of Sciences, 457 Zhongshan Road, 116023 Dalian, China
e-mail: taozhang@dicp.ac.cn

P. Gao
Graduate School of Chinese Academy of Sciences, 100039 Beijing, China

Our results showed that Ru nanoparticles prepared with this one-pot method were highly dispersed on the mesoporous carbons, and the Ru-OMC exhibited high activities and selectivities toward unsaturated alcohol in the hydrogenation of cinnamaldehyde.

2 Experimental

2.1 Catalyst Preparation

The preparation of Ru-OMC was similar to that of Ir-OMC [15] with a key modification. In detail, 1.65 g of resorcinol was dissolved in a solution containing 1.25 g of F127 and 10 g of ethanol/water (1/1 vol%) under stirring. When a light brown solution was formed, 0.2 g of HCl (37 wt%) was added as a catalyst. After stirring for 2 h, 1.25 g of formaldehyde (37%) was dropped into the above solution. Followed by additional 2 h of stirring, a required amount of $RuCl_3$ was added. Then, the mixture was kept standing until it turned cloudy and began to separate into two layers. This two-phase mixture was further kept aging for 96 h. Subsequently, the upper layer was discarded while the lower polymer-rich phase was stirred overnight until a sticky monolith was formed. Finally, the monolith was cured at 85 °C for 48 h and pyrolyzed under N_2 atmosphere at 800 °C for 3 h at a heating rate of 1 °C/min. To be noted, if the $RuCl_3$ was added together with HCl as described in Ref. [15, 16], the resulting Ru-OMC would have large Ru particles. The denotations and chemical compositions of these samples are shown in Table 1.

2.2 Catalyst Characterizations

Nitrogen adsorption-desorption isotherms were obtained on a Micromeritics ASAP 2010 apparatus at −196 °C. Prior to the measurements, the samples were degassed at 250 °C for 4 h. The Brunauer–Emmett–Teller (BET) method was used to calculate the specific surface areas. Pore size distributions were derived from the desorption branches of the isotherms using the Barrett–Joyner–Halen (BJH) method. Powder X-ray diffraction (XRD) patterns were recorded with a PANalytical X'Pert-Pro powder X-ray diffractometer using Cu Kα radiation. Transmission electron microscopy (TEM) was conducted on a JEOL 2000 EX electronic microscope with an accelerating voltage of 120 kV. Chemical compositions of the Ru-OMC were determined by inductively coupled plasma spectrometer (ICP–AES) on an IRIS Intrepid II XSP instrument (Thermo Electron Corporation).

2.3 Hydrogenation Reaction

The hydrogenation of cinnamaldehyde (CMA) was carried out in a 300 mL stainless steel autoclave (Parr 5500 reactor) at 100 °C, 3 MPa of H_2, and a stirring speed of 1000 rmp. In each experiment, 0.1 g of a catalyst, 80 mL of isopropanol, and 2.0 mL of CMA was used. The reaction was monitored by sampling and analysis at regular intervals to determine the conversion and selectivity. The reaction products were analyzed by gas chromatography (Agilent 6890) equipped with a flame ionization detector (FID) and a 0.25 mm × 30 m FFAP capillary column.

3 Results and Discussion

3.1 Formation of Mesoporous Structure

Since all the Ru-OMC samples present similar N_2 sorption isotherms, we here illustrate only one typical N_2 adsorption-desorption isotherm and the corresponding pore size distribution (Fig. 1), and the textural properties of the samples with different Ru contents are summarized in Table 1. Similar to the previously reported Ir-OMC, the Ru-OMC presents typical type IV isotherm with a well-defined hysteresis loop, indicating its well ordered mesostructure. It has a very narrow pore size distribution,

Table 1 Textural properties of the Ru-OMC samples

Sample	S_{BET} (m^2/g)	V_P[a] (cm^3/g)	V_{meso} (cm^3/g)	V_{micro}[b] (cm^3/g)	D_p[c] (nm)	*d*-Value (nm)	Ru content[d] (wt%)
0.47Ru-OMC	743	0.65	0.55	0.17	4.5	10.4	0.47
0.36Ru-OMC	693	0.63	0.51	0.15	4.2	10.0	0.36
0.66Ru-OMC	683	0.62	0.53	0.14	4.5	10.2	0.66
0.97Ru-OMC	722	0.63	0.51	0.17	4.6	11.5	0.97
OMC	734	0.66	0.56	0.16	4.5	9.9	–

[a] The total pore volume was determined by adsorption volume at $P/P_0 = 0.99$

[b] The micropore volume was determined according to the *t*-plot method

[c] The average pore diameter was calculated based on the BJH method

[d] Ru contents were determined by ICP analysis

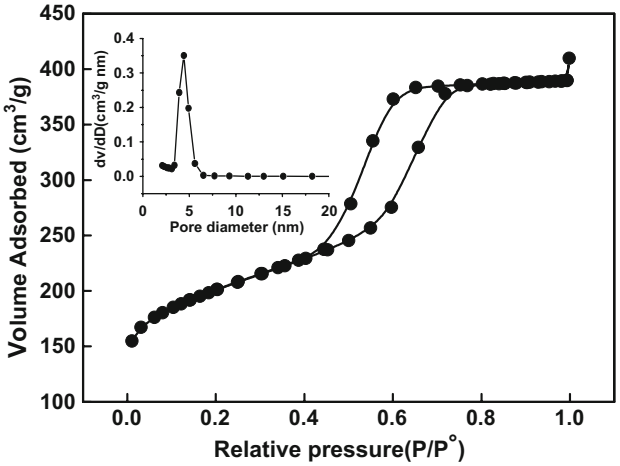

Fig. 1 N_2 adsorption-desorption isotherm and the corresponding pore size distribution of the 0.36Ru-OMC samples

centering at ~4.5 nm. It is noted that with a rise of the Ru content, both the BET surface areas and the pore volumes almost remain constant ($S_{BET} = 700$ m^2/g and $V_P = 0.63$ m^3/g). This result implies no pore-blocking occurring upon the incorporation of Ru.

To further demonstrate the formation of ordered mesoporous structure, we performed XRD and TEM characterizations on the Ru-OMC samples. As shown in Fig. 2, all the samples present a diffraction peak at $2\theta = 0.5$–$1°$ (inset) which can be indexed as (100) reflection of a hexagonal mesostructure, and the peak seems to have a shift toward the lower angles with an increase of the Ru content. The enlarged *d*-value (Table 1) in the Ru-containing samples suggests that the framework shrinkage occurring during the pyrolysis were alleviated more or less by the incorporation of Ru. The same conclusion was also

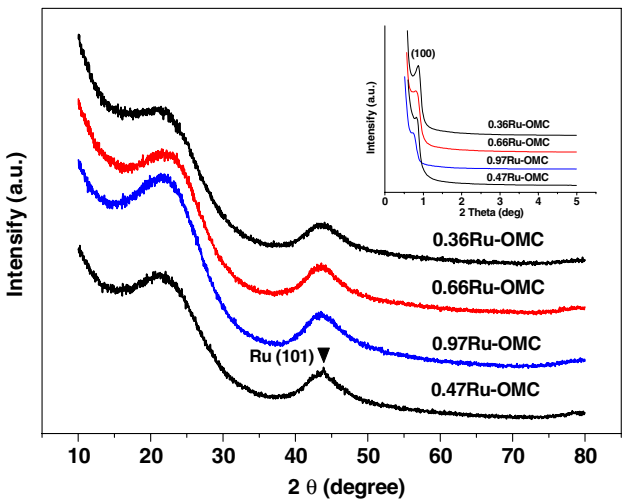

Fig. 2 Wide-angle XRD patterns of the Ru-OMC samples with different Ru contents (inset: the low-angle XRD patterns)

arrived at in Ir-OMC samples [15]. In the wide angle range, two broad diffraction peaks at 21.7° and 43.6° characteristic of amorphous carbon appeared, and no any other peaks assignable to Ru could be observed. This may be due either to the low content of Ru or to the very small particle size. To address this question, we prepared another Ru-OMC sample (0.47Ru-OMC, prepared with the same method as that for Ir-OMC [15]) with a comparable Ru content but a larger particle size. Its XRD pattern shows a discernable peak at 44° which can be indexed as (101) reflection of hexagonal Ru metal (JCPDS 06-0663). This result implies that our Ru-OMC samples prepared by a modified procedure should have a very small Ru particle size.

Consistent with the XRD results, the TEM images in Fig. 3 clearly show that the Ru-OMC samples have well ordered hexagonal mesostructures. Arrays of long 1-D channels are clearly observed. Ru particles are hardly discernible on the 0.36Ru-OMC and 0.66Ru-OMC samples. However, on the 0.97Ru/OMC sample, very small (<2 nm) and highly dispersed Ru nanoparticles can be clearly observed. In contrast with these samples, the 0.47Ru-OMC which was prepared with the same procedure as that for Ir-OMC [15] presents large and poorly dispersed Ru particles, and most of the particles are in the range of 5–10 nm. Evidently, our modified procedure yielded very small and highly dispersed Ru nanoparticles. According to Ref. [17, 21, 22] and our own previous work [15, 16], these Ru particles should be imbedded in the carbons. The key for the modified procedure is the adding time of the Ru precursor. Considering that the initial reduction potential of Ru^{3+} is lower than that of Ir^{4+}, the Ru precursor must be added after all the formaldehyde was consumed for polymerization with resorcinol so that it cannot be reduced to Ru^0 by the formaldehyde. Once the Ru^{3+} had already been reduced by the formaldehyde, the following pyrolysis would make these particles agglomerate seriously, as in the case of 0.47Ru-OMC. Therefore, our modified procedure ensured the reduction of Ru^{3+} occurring during the pyrolysis with the carbon itself as the reducing agent.

3.2 Hydrogenation of CMA

The selective hydrogenation of α,β-unsaturated aldehydes to their corresponding unsaturated alcohols is of great importance in the synthesis of fine chemicals, and it is also considered as a good model reaction in correlating the catalytic behaviors with microstructures of heterogeneous catalysts [23–28]. The presence of two conjugated double bonds in α,β-unsaturated aldehydes allows two competitive hydrogenation routes: the hydrogenation of the C=C bond to the saturated aldehydes and the hydrogenation of the C=O bond to the unsaturated alcohols (as shown in

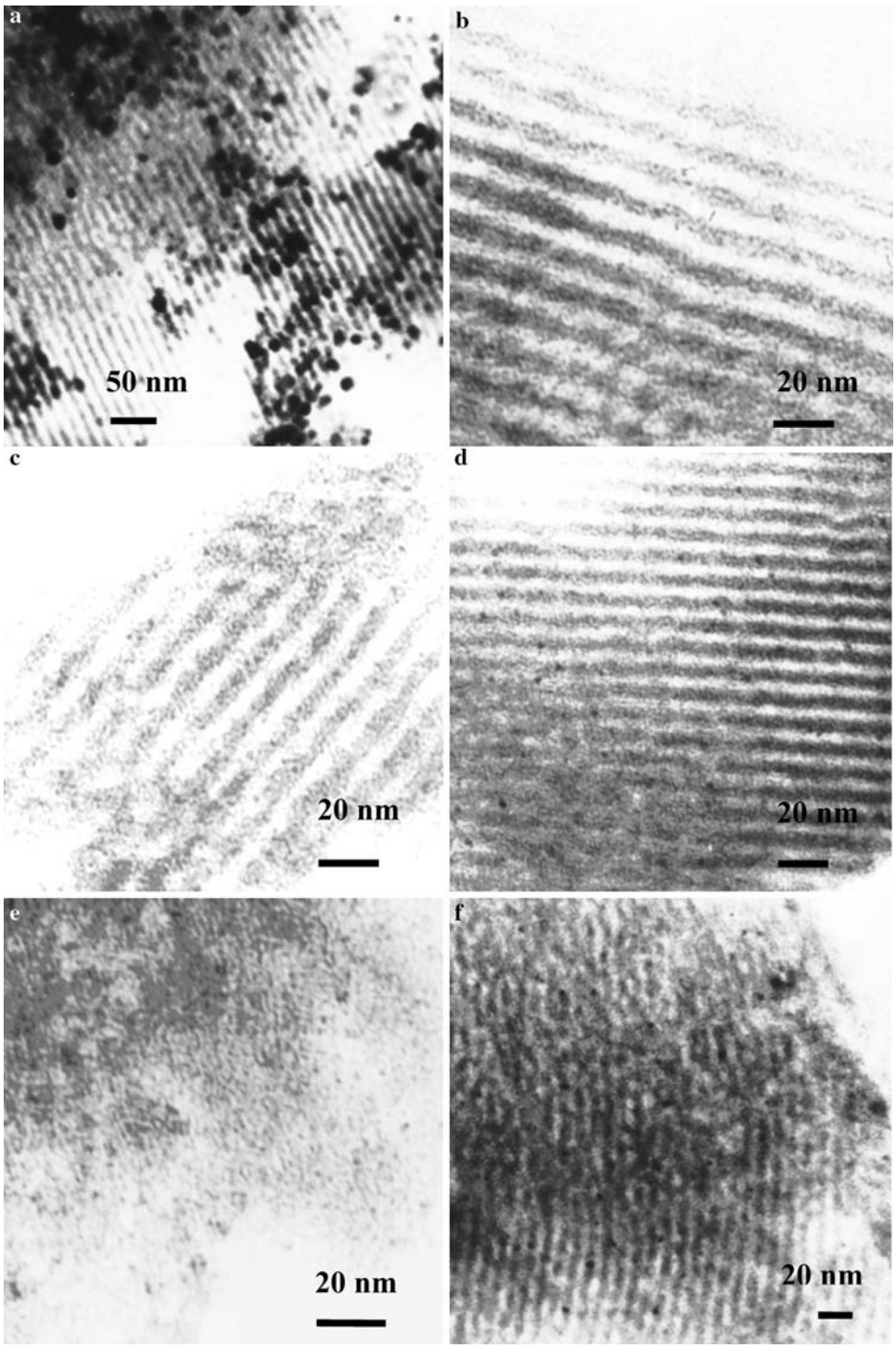

Fig. 3 TEM images of the 0.47Ru-OMC (**a**), 0.36Ru-OMC (**b**), 0.66Ru-OMC (**c**), 0.97Ru-OMC (**d**), Ru/AC (**e**) and Ru/OMC (**f**)

Scheme 1). Unfortunately, the selective hydrogenation of the C=O bond is thermodynamically unfavored, which requires a suitable catalyst favoring the C=O hydrogenation while keeping the C=C bond intact, in order to obtain the desired unsaturated alcohols. In the past years, Pt- and Ru-based catalysts have been intensively studied for this type of reaction and an electronic modification with a second metal is often required to obtain an improved selectivity [25–28].

In this work, we used the above-synthesized Ru-OMC catalysts for the hydrogenation of CMA. For comparison, a Ru/AC, as well as a Ru/OMC which was prepared by conventional impregnation procedure was also investigated for this reaction. The Ru content was 4.90 wt% for Ru/AC

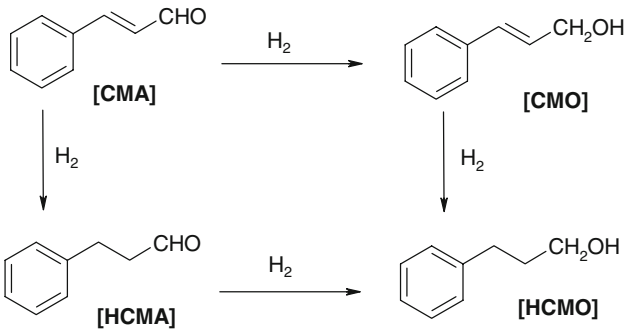

Scheme 1 Cinnamaldehyde hydrogenation reaction pathways. CMA, cinnamaldehyde; CMO, cinnamyl alcohol; HCMA, hydrocinnamaldehyde; and HCMO, hydrocinnamyl alcohol

and 2.0 wt% for Ru/OMC, respectively. The TEM images in Fig. 3e and f reveal that the Ru particles are also well dispersed for the two samples. The CMA conversion and the product distribution over the Ru/AC, Ru/OMC, and our one-pot synthesized Ru-OMC catalysts are displayed in Fig. 4. As shown in Fig. 4a, the main product for the CMA hydrogenation over our Ru-OMC catalyst is CMO arising from the C=O double bond hydrogenation, whereas the selectivities to the hydrogenation of C=C bond (HCMA) and that of both the C=O and C=C bonds (HCMO) are relatively low (below 10%). An unconventional behavior of the Ru-OMC is that the selectivity to CMO seems to remain constant at 54% with the reaction time, even at the CMA conversion near to 100%. This is very different from the literature-reported Ru/C [19]. On the contrary, when the Ru/AC or Ru/OMC which was prepared by conventional impregnation method was used as the catalyst (Fig. 4b, c), the main products were HCMA and HCMO, the selectivity to CMO was very low. In particular, with an increase of the reaction time, the complete hydrogenation predominated, reflected by the high selectivity to HCMO at a high conversion of CMA. Apparently, the Ru-OMC samples prepared by one-pot procedure exhibited superior selectivities toward C=O hydrogenation over both the Ru/AC and Ru/OMC samples prepared by conventional impregnation. It should be pointed out that the total sum of the product selectivities in Fig. 4 is far less than 100% because substantial amounts of acetals resulting from the condensation between aldehydes (CMA and HCMA) and the solvent isopropanol were also detected. In addition, other unidentified compounds were also detected, but their amount was negligible. Table 2 lists the conversion and selectivity at different reaction time on the three Ru-OMC catalysts with varied Ru content. Both the CMA conversion and the CMO selectivity were enhanced when the Ru content was increased from 0.36 to 0.97 wt%. The selectivity improvement can be explained by the size effect. It is known that the selectivity to CMO increases with

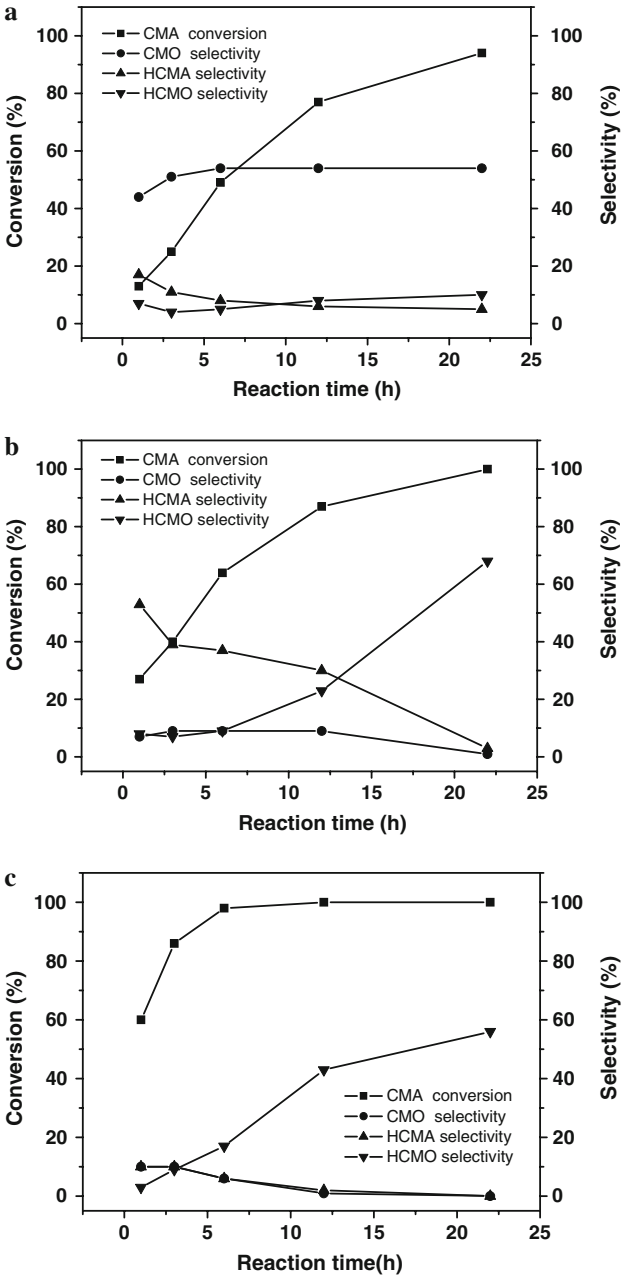

Fig. 4 The conversion of CMA and the selectivity to each product as a function of the reaction time for 0.97Ru-OMC (**a**), 4.9Ru/AC (**b**), and 2.0Ru/OMC (**c**)

increasing metal particle size since steric hindrance prevents adsorption and activation of the C=C bond on the surface of metal particles. Our TEM examinations clearly show that the Ru particle size decreases in the order of 0.47Ru-OMC > 0.97Ru-OMC > 0.36Ru-OMC, which is in good agreement with the selectivity trend. It should be emphasized that in our Ru-OMC catalyst samples, the Ru content is very low. Even though, the initial conversion of CMA on these samples is comparable to that on the Ru/AC which has a higher Ru content (4.9 wt%). That means our

Table 2 CMA conversions (conv.) and selectivities to CMO (selec.) obtained over the different Ru-containing samples

Samples	1 h Conv./selec. (%)	3 h Conv./selec. (%)	6 h Conv./selec. (%)	12 h Conv./selec. (%)	22 h Conv./selec. (%)	TOF at 1 h (s^{-1})
0.47Ru-OMC	7/45	12/52	17/54	31/58	52/60	0.664
0.36Ru-OMC	16/40	25/46	37/49	61/52	86/51	0.198
0.97Ru-OMC	13/44	25/51	49/54	77/54	94/54	0.120
4.9Ru/AC	27/7	40/9	64/9	87/9	100/1	0.049
2.0Ru/OMC	60/10	86/10	98/6	100/1	100/0	–

Ru-OMC catalysts may have a high intrinsic activity for the hydrogenation of CMA. According to the initial conversion and the particle size of Ru, we calculated turnover frequencies (TOFs) of the catalysts. From Table 2, one can see that the TOFs of our Ru-OMC catalysts are at least 2.5-fold higher than that of the Ru/AC. Especially for the 0.47Ru-OMC, its intrinsic activity is 14-fold compared with the Ru-AC. The origin for such a high activity of the Ru-OMC is not yet clear. Recently, Su et al. [17] reported that Ru nanoparticles prepared on various carbon-based supports by a thermal reduction method displayed a remarkably high catalytic activity and stability in benzene hydrogenation (up to 3–24-fold compared with Ru catalysts prepared by traditional hydrogen reduction method). They attributed such a high activity to the intimate interfacial contact between Ru particles and the carbon support. In our one-pot synthesis procedure, the formation of Ru nanoparticles also originated from the thermal reduction with the carbon itself as the reducing agent, together with the formation of mesoporous carbon structure. Moreover, the Ru precursor had been entrapped in the polymer network before they were subjected to pyrolysis, which would create strong interaction with the carbon support during the pyrolysis. According to our previous work [15, 16], such one-pot formed Ru nanoparticles were mainly imbedded in or anchored on the carbon walls. Therefore, the intimate contact and strong interaction between the Ru nanoparticles and the carbon support are possibly responsible for the high catalytic activity and selectivity to the CMO in the hydrogenation of CMA. To be noted, with the ever increasing price of precious metals, enhancing the catalytic activity of a precious metal catalyst while remaining its selectivity unchanged will become more and more desirable in the future.

On the other hand, we also investigated the possible confinement effect of the mesopores. By comparing with the Ru/OMC as well as Ru/MCM-41 [18], one can see that despite its high activity (the CMA conversion attained 60% after 1 h-run), the selectivity to the CMO was below 10% over the Ru/OMC. This is because the Ru/OMC prepared by conventional impregnation and H_2-reduction method had a relatively weak interaction between Ru and the OMC support when comparing with our one-pot synthesized Ru-OMC samples. On the other hand, the Ru/MCM-41 [18] samples prepared with different methods were always inferior to our present Ru-OMC in terms of activity and selectivity to CMO. Accordingly, we can conclude that the steric hindrance imposed by the nanopores has little effect on the activity and selectivity of the Ru-OMC. Instead, the intimate contact and strong interaction between Ru nanoparticles and the carbon support resulting from the one-pot synthesis method should be responsible for the superior performance of the Ru-OMC catalysts.

4 Conclusion

In summary, we have prepared Ru-containing mesoporous carbons with highly ordered structures by the one-pot synthesis method. The particle size of Ru could be tuned by changing the adding time and the amount of the Ru precursor during the synthesis. This one-pot synthesis gave rise to the intimate interfacial contact between the Ru particles and the carbon support and also created strong interaction between them. Thereby, the resulting Ru-OMC catalysts exhibited very high activities (2–14-fold compared with the Ru/AC which were prepared by impregnation method) and selectivities toward CMO in the hydrogenation of CMA.

Acknowledgments Supports from National Science Foundation of China (NSFC) for Distinguished Young Scholars (No. 20325620) and NSFC grants (No. 20673116, 20773124 and 20773122) are gratefully acknowledged.

References

1. Yang Z, Xia Y, Mokaya R (2007) J Am Chem Soc 129:1673
2. Zeng JH, Su FB, Lee JY, Zhou WJ, Zhao XS (2006) Carbon 44:1713
3. Baughman RH, Zakhidov AA, de Heer WA (2002) Science 297:787
4. Job N, Pereira MFR, Lambert S, Cabiac A, Delahay G, Colomer J-F, Marien J, Figueiredo JL, Pirard J-P (2006) J Catal 240:160
5. Zhou H, Zhu S, Hibino M, Honma I, Ichihara M (2003) Adv Mater 15:2107

6. Hartmann M, Vinu A, Chandrasekar G (2005) Chem Mater 17:829
7. Joo SH, Choi SJ, Oh I, Kwak J, Liu Z, Terasaki O, Ryoo R (2001) Nature 412:169
8. Ryoo R, Joo SH, Kruk M, Jaroniec M (2001) Adv Mater 13:677
9. Liang CD, Dai S (2004) Angew Chem Int Ed 43:5785
10. Liang CD, Dai S (2006) J Am Chem Soc 128:5316
11. Meng Y, Gu D, Zhang FQ, Shi YF, Yang HF, Li Z, Yu CZ, Zhao DY (2005) Angew Chem Int Ed 44:7053
12. Zhang FQ, Meng Y, Gu D, Yan Y, Yu CZ, Tu B, Zhao DY (2005) J Am Chem Soc 127:13508
13. Meng Y, Gu D, Zhang FQ, Shi YF, Cheng L, Feng D, Wu ZX, Chen ZX, Wan Y, Stein A, Zhao DY (2006) Chem Mater 18:4447
14. Huang Y, Cai HQ, Yu T, Zhang FQ, Zhang F, Meng Y, Gu D, Wan Y, Sun XL, Tu B, Zhao DY (2007) Angew Chem Int Ed 46:1089
15. Gao P, Wang AQ, Wang XD, Zhang T (2008) Chem Mater 20:1881
16. Wang H, Wang AQ, Wang XD, Zhang T (2008) Chem Commun 2565
17. Su FB, Lv L, Lee FY, Liu T, Cooper AI, Zhao XS (2007) J Am Chem Soc 129:14213
18. Kumar N, Mäki-Arvela P, Hajek J, Salmi T, Murzin DY, Heikkilä T, Laine E, Laukkanen P, Väyrynen J (2004) Microporous Mesoporous Mat 69:173
19. Hájek J, Kumar N, Mäki-Arvela P, Salmi T, Murzin DY, Paseka I, Heikkilä T, Laine E, Laukkanen P, Väyrynen J (2003) Appl Catal A Gen 251:385
20. Vu H, Goncalves F, Philippe R, Lamouroux E, Corrias M, Kihn Y, Kack P, Serp P (2006) J Catal 240:18
21. Lu AH, Li WC, Hou ZS, Schüth F (2007) Chem Commun 1038
22. Liu SH, Lu RF, Huang SJ, Lo AY, Chien SH, Liu SB (2006) Chem Commun 3435
23. Gallezot P, Fendler A, Richard D (1991) In: Pascoe WE (ed) Catalysis of organic reactions. Marcel Dekker, Inc., New York, p 1
24. Coq B, Figueras F (1998) Coord Chem Rev 178
25. Nahata N, Goncalves F, Pereira MFR, Figueiredo JL (2008) Appl Catal A Gen 339:159
26. Li Y, Zhu PF, Zhou RX (2008) Appl Surf Sci 254:2609
27. Gallezot P, Richard D (1998) Catal Rev Sci Eng 40:81
28. Mäki-Arvela P, Hájek J, Salmi T, Murzin DY (2005) Appl Catal A Gen 292:1